Kovove Mater. 55 2017 191–194
DOI: 10.4149/km_2017_3_191

Mechanical properties of friction stir welded 2024 aluminum alloy and precipitated phases in stir zone

Y. B. Zhang[1]*, C. Y. Du[2], J. N. Li[1]

[1] *School of Materials Science and Engineering, Shandong Jianzhu University, Jinan 250101, P. R. China*
[2] *School of Materials Science and Engineering, Shandong University, Jinan 250061, P. R. China*

Received 17 March 2016, received in revised form 17 July 2016, accepted 19 July 2016

Abstract

2024 aluminum alloy sheets in T4 temper were welded successfully by friction stir welding (FSW) technique. When the welding travel speed was 300 mm min^{-1}, tensile strength reached a maximum value (294 MPa). The precipitated phase is mainly metastable U(AlCuMg) of reinforced phases in thermo-mechanically affected zone (TMAZ). Lots of the $AlCu_3$ black particles precipitated on the grain boundary of TMAZ. However, a large number of Cu_2Mg black granular precipitates were observed in the WN region.

Key words: friction stir welding, welding, metals and alloys

1. Introduction

The light alloys, such as Al-Cu-Mg and Al-Ti-Cu alloys are widely used in the aerospace, automobile industry and machine parts [1, 2]. However, it is often difficult to obtain the weld without hot cracking, porosity or distortions by conventional fusion welding techniques since the hardenable aluminum alloys (Al-Cu-Mg) are in a loss in strength and ductility. At present, FSW, a solid state joining method has been used for those aluminum alloys difficult to join by fusion welding [3, 4].

Corrosion resistance and weldability of 2024 aluminum alloys are relatively poor. In recent years, the FSW technique was used to join the butt welds for the 2024 aluminum alloys. Therefore, butt friction stir welds with high quality can be obtained [5]. The correlation between the microstructure characteristics of the weld, especially in the weld nugget (WN) region and TMAZ, is one of the most important issues in FSW optimization. The WN region was thought to experience a “continuous” dynamic recrystallization (CDRX) process. However, in TMAZ the material has been plastically deformed by the tool, and the heat flux has also exerted some influence on the material. Extensive deformation is present in this zone. The precipitated phase in the central stir zone (WN and TMAZ) has an important effect on the mechanical properties of FSW joints. At present, Jones and Genevois [6, 7] analyzed the correlation between microstructure and microhardness of FSW joint for AA2024-T351 aluminum alloy by using transmission electron microscopy (TEM). In this study, the mechanical properties of FS weld were measured by micro sclerometer and tensile testing machine of CSS-1100 type. The precipitated phases in the TMAZ were observed and analyzed using a transmission electron microscopy (TEM) technique.

2. Experimental

The examined joined sheets of 2024-T4 aluminum alloys (T4 temper) had dimensions of 150 mm × 60 mm × 3 mm. The test sheets were treated by acetone solution. Then, two 3 mm thick sheets were butt welded by using an FSW technique. The welding direction was parallel to the rolling direction of the sheets. The tool rotational speed and travel speed were 475 rpm and 150–375 mm min^{-1}, respectively.

The 2024-T4 aluminum alloy sheets were welded successfully using FSW technique. A series of specimens was cut, and then these specimens were made into metallographic samples. The samples were etched

*Corresponding author: tel.: 13854112137; fax: +86-531-86361267; e-mail address: yuy2332@126.com

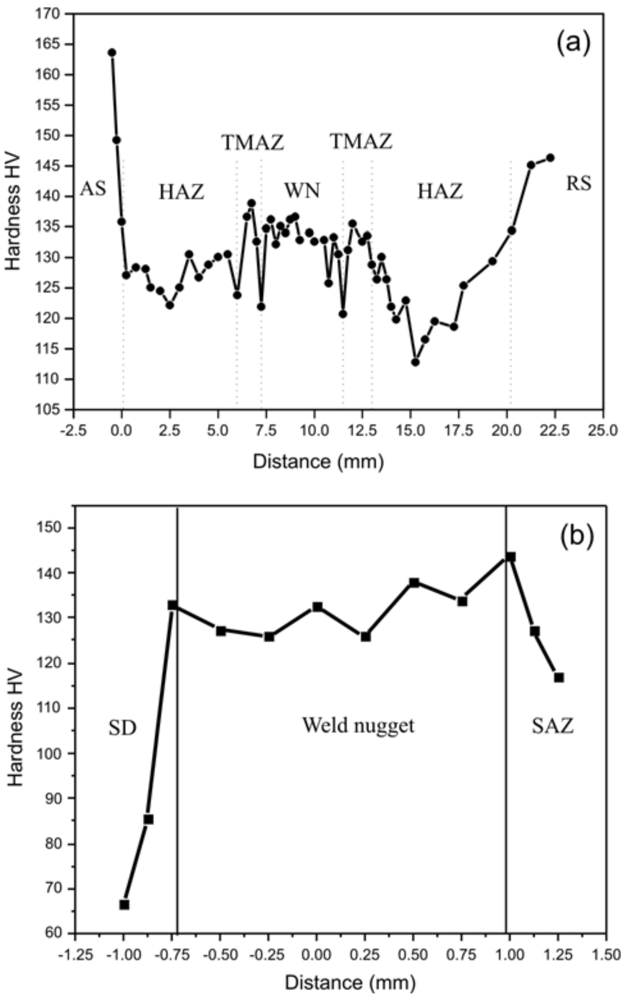

Fig. 1. Microhardness distribution in the weld of FSW joint: (a) microhardness in the weld and (b) microhardness in weld nugget.

using mixed solution 1.0 % HF + 1.5 % HCl + 2.5 % HNO_3 + 95 % H_2O (vol.%). Then, the etched samples were cut into foils by line cutting machine. A double jet electro-polishing technique was used for thin-foil preparation in an electrolyte, containing HNO_3 and CH_3OH (1 : 2) at –20 ℃. Microstructural analysis was carried out on a JEOL 2011 FX instrument with a W-filament operated at 200 kV.

3. Results and analysis

The microhardness in stir zone of the 2024 aluminum alloys was measured using a Shimadzu type micro sclerometer, using 100 g loading and a load time of 10 s. The test results are shown in Fig. 1. In Fig. 1a, the microhardness was measured from advancing side to retreating side along weld cross section. However, the microhardness was measured from bottom swirl defects (SD) to upper shoulder affected zone (SAZ), see Fig. 1b.

According to Fig. 1a, the hardness value from base metal to weld zone decreased gradually. The hardness value was about 120 HV in the HAZ. The hardness value toward the TMAZ increased gradually and reached 140 HV. Finally, the hardness value decreased gradually in WN. However, the microhardness distribution in this region was steady. The test results indicated that the hardness value near the interface of WNZ/TMAZ was approximate. However, the hardness value near the interface of HAZ/TMAZ was greatly different. This difference was related to the precipitated phases and welding thermal cycle in the stir zone. The difference of hardness distribution induces different shrinkage distortions of weld metal near the interface of HAZ/TMAZ during the cooling. As a result, larger residual stress concentration in this region occurs, making this region a weaker region of strength distribution for FSW joints.

The microhardness distribution along the thickness direction of FS weld over the weld nugget is shown in Fig. 1b. According to Fig. 1b, the hardness value of bottom swirl defects (SD) zone is lower than that of weld nugget and upper shoulder affected zone (SAZ). Since the weld metal of SD zone has not contact with the tool pin, the welding temperature in this region is lower. However, the weld metal in this region produced plastic deformation as the tool pin rotated. Thus, the recrystallization phenomenon was not induced, the microhardness in this region decreased obviously.

The tensile strength and fracture morphology of joints reflect effectively mechanical properties of FS weld for 2024 aluminum alloys. Figure 2 shows the test results of tensile strength for FSW joints of 2024 aluminum alloys. The rotational speed of tool pin was

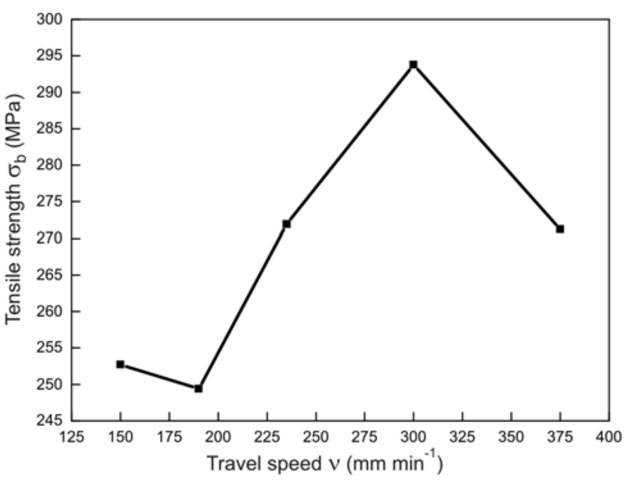

Fig. 2. Relationship between tensile strength and travel speed of FSW joint.

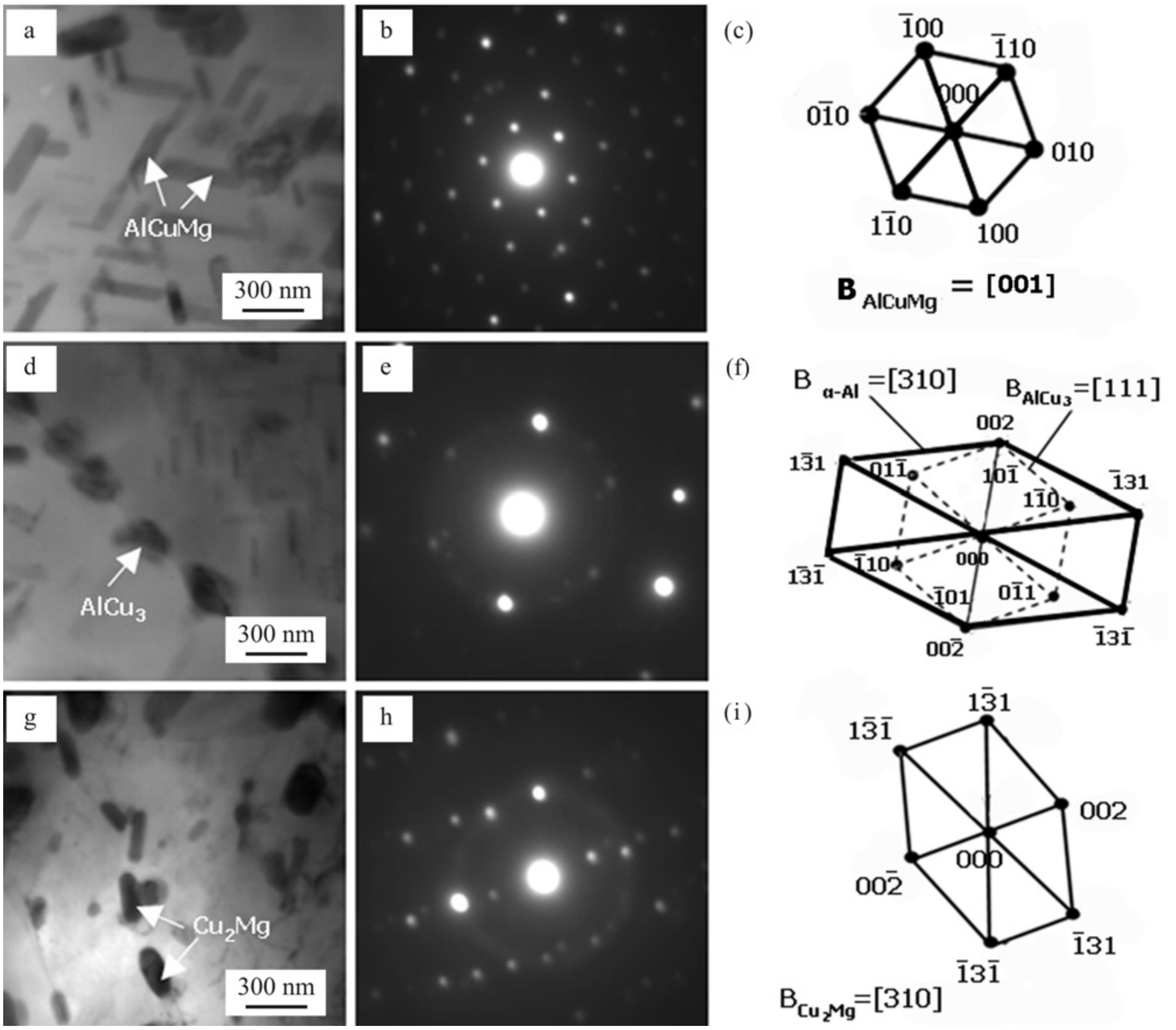

Fig. 3. TEM image and corresponding EDP of the AlCuMg [001] precipitated phase in TMAZ: (a) TEM image, (b) EDP, (c) schematic index diagram of panel; TEM image and corresponding EDP of the $AlCu_3$ [111] precipitated phase and α-Al [310] in TMAZ: (d) TEM image, (e) EDP, (f) schematic index diagram of panel; TEM image and corresponding EDP of Cu_2Mg [310] precipitated phase in WN region: (g) TEM image, (h) EDP, (i) schematic index diagram of panel.

475 rpm, and the travel speed along weld was 150–375 mm min^{-1}.

According to Fig. 2, the tensile strength of joints increased gradually with the increase of welding travel speed. When the welding travel speed was 300 mm min^{-1} the tensile strength reached the maximum value (294 MPa). It is about 70 % of tensile strength for 2024 aluminum alloys. However, with the further increase of welding travel speed, the tensile strength of joints decreased gradually. The tensile strength of joints was about 60 % of that of the 2024 aluminum alloys when the welding travel speed was 190 mm min^{-1}.

Precipitates in inner grain and grain boundary of central weld were observed and analyzed by TEM. In the experiment, the sample with maximum tensile strength was selected (rotational speed and travel speed were 475 rpm and 300 mm min^{-1}, respectively). TEM morphology and corresponding electron diffraction pattern (EDP) of precipitated phases in the TMAZ can be seen in Figs. 3a–c and Figs. 3d–f. Figures 3g–i show the TEM morphology and corresponding electron diffraction pattern of precipitated phase in WN.

In TMAZ, the precipitated phase is mainly U-phase (AlCuMg) (see Fig. 3a). According to Figs. 3b and 3c, the zone axis of U(AlCuMg) is $B = [001]$. The AlCuMg has a close-packed hexagonal (hcp) structure, and the lattice constant is $a = 0.509$ nm. In the Al-Cu-Mg alloys (2024-T4), the constituents that can exist in equilibrium with Al-rich solid solution are the two binary phases, $\beta(Mg_2Al_3)$ and $\theta(CuAl_2)$, and the two ternary phases designated S and T, which are also reinforced phases [8, 9]. There is no report about U-phase observation in FSW joint. However, during FSW of 2024 aluminum alloys, the fine S' (S) precipitates were usually formed in TMAZ. The hardness minimum was thought to be due to the dissolution of the fine S-phase occurring towards the outer edge of HAZ. The hardness maximum between these two minima was seen to be due to the presence of very fine S-phase.

The U-phase (AlCuMg) found in the TMAZ region may be in relation to the FSW technology. In this FSW technology, the increase of temperature in TMAZ region induces the dissolution of GP zones (θ-$CuAl_2$, β-Mg_2Al_3). Then, supersaturated solid solution continues precipitating: $\alpha \rightarrow$ GP zone $\rightarrow U' \rightarrow U$(AlCuMg). The U-phase formed in the TMAZ was not in equilibrium with the aluminum-rich phase in the ternary alloys and was also a metastable phase. As a result, this phase may be the major reason to induce the hardness difference in the HAZ/TMAZ.

Some of the black granular $AlCu_3$ were aggregated and precipitated on the grain boundary of the TMAZ (see Fig. 3d). As shown in Figs. 3e and f, the zone axis of $AlCu_3$ is $B = [111]$. $AlCu_3$ has a body-centered cubic (bcc) structure, and lattice constant is $a = 0.295$ nm. The lattice orientation between $AlCu_3$ and α-Al is $(10\bar{1})_{AlCu_3} \parallel (001)_{\alpha\text{-Al}}$. The precipitated phase of $AlCu_3$ gathering on the grain boundary may increase the brittleness of the FSW weld.

The results indicate that a large number of black granular precipitation particles (Cu_2Mg) appear in the WN region (see Figs. 3g and 3h). The zone axis of Cu_2Mg is $B = [310]$. The Cu_2Mg has a face-centered cubic (fcc) structure, and lattice constant is $a = 0.699$ nm (see Fig. 3i). The Cu_2Mg was mainly precipitated in the crystal grain, and little particles were precipitated near the grain boundary. According to Figs. 3g and 3h, there are some complex mixed dislocations in the crystal grain.

4. Conclusions

In summary, the 2024 aluminum alloy sheets in the T4 temper were welded successfully by the FSW techniques. The hardness value near the interface of HAZ/TMAZ was greatly different. This difference was related to the precipitated phases and welding thermal cycle in stir zone. The hardness value of bottom swirl defects (SD) is lower than that of weld nugget and upper shoulder affected zone (SAZ). The tensile strength of joints increased gradually with the increase of welding travel speed. When the welding travel speed was 300 mm min^{-1}, the tensile strength reached the maximum value 294 MPa. The precipitated phase is mainly U(AlCuMg) of metastable phases in the TMAZ using TEM analysis. The AlCuMg has a close-packed hexagonal (hcp) structure, and lattice constant is $a = 0.509$ nm. Some of the black granular $AlCu_3$ were aggregated and precipitated on the grain boundary of the TMAZ. The $AlCu_3$ has a body-centered cubic (bcc) structure, and lattice constant is $a = 0.295$ nm. The lattice orientation between $AlCu_3$ and α-Al is $(10\bar{1})_{AlCu_3} \parallel (001)_{\alpha\text{-Al}}$. The precipitated phase of $AlCu_3$ gathering on the grain boundary may increase the brittleness of FSW weld. A large number of black granular precipitated particles, Cu_2Mg, appear in the WN region.

Acknowledgement

This work was financially supported by the National Natural Science Foundation of China (Grant No. 50874069).

References

[1] Ferragut, R.: Physica B: Condensed Matter, *407*, 2012, p. 2676. doi:10.1016/j.physb.2012.02.008
[2] Li, J. N., Yu, Y. J., Chen, C. Z., Gong, S. L.: J. Phys. Chem. C, *117*, 2013, p. 4568. doi:10.1021/jp311138f
[3] Ghosh, M., Kar, A., Kumar, K., Kailas, S. V.: Mater. Technol. Adv. Perform. Mater., *27*, 2012, p. 169. doi:1179/175355509X12608916825994
[4] Murr, L. E., Li, Y., Trillo, E. A., McClure, J. C.: Mater. Technol. Adv. Perform. Mater., *15*, 2000, p. 37.
[5] Staron, P., Kocak, M., Williams, S., Wescott, A.: Physica B, *350*, 2004, p. E491. doi:10.1016/j.physb.2004.03.128
[6] Jones, M. J., Heurtier, P., Desrayaud, C., Montheilet, F., Allehaux, D., Driver, J. H.: Scripta Mater., *52*, 2005, p. 693. doi:10.1016/j.scriptamat.2004.12.027
[7] Genevois, C., Deschamps, A., Denquin, A., Doisneau-Cottignies, B.: Acta Mater., *53,* 2005, p. 2447. doi:10.1016/j.actamat.2005.02.007
[8] Tomida, S., Nakata, K., Saji, S., Kubo, T.: Surf. Coat. Technol., *142–144*, 2001, p. 585. doi:10.1016/S0257-8972(01)01172-0
[9] Wen, W., Liu, W. C., Morris, J. G.: Mater. Sci. Eng. A, *380*, 2004, p. 191. doi:10.1016/j.msea.2004.03.072